

# Lawrence Berkeley National Laboratory

## LBL Publications

### Title

Nanoparticle surfactants and structured liquids

### Permalink

<https://escholarship.org/uc/item/9qw8x2fd>

### Journal

Colloid and Polymer Science, 299(3)

### ISSN

0303-402X

### Authors

Sun, Shuyi  
Liu, Tan  
Shi, Shaowei  
[et al.](#)

### Publication Date

2021-03-01

### DOI

10.1007/s00396-020-04724-2

Peer reviewed

# Nanoparticle surfactants and structured liquids

Shuyi Sun<sup>1</sup> & Tan Liu<sup>1</sup> & Shaowei Shi<sup>1</sup> & Thomas P. Russell<sup>1,2,3</sup>

## Abstract

Materials are usually classified as solids or liquids, based on their structural stability, dynamic response, and rheological properties. Structured liquid, a new state of matter, has attracted much attention in recent years. Different with either solid or liquid, structured liquid combines the desirable characteristics of fluids with the structural stability of a solid, showing a myriad of potential applications in encapsulation, biphasic reactors, and programmable liquid constructs. Here, a brief review is given, by introducing a new strategy to structure liquids based on the formation, assembly, and jamming of nanoparticle surfactants (NPSs) at liquid-liquid interfaces. The interfacial packing of the NPSs can be effectively manipulated using external triggers, endowing the structured liquids with adaptiveness and responsiveness to changes in their external environment.

**Keywords** Nanoparticle surfactants · Interfacial assembly · Structured liquids

## Introduction

When it comes to liquids, the first words that come to mind are soft, flowing, and shapeless. These properties distinguish liquids from solids, which, in turn, make liquids difficult to be processed and molded. Imagine how wonderful it would be if liquids could be shaped as desired. In this case, the structures of liquids can be manipulated to complex geometries and can be further used for the construction of complex liquid devices for charge and mass transduction, compartmentalized reaction, encapsulation, and delivery. Recently, by taking advantage of the jamming of colloidal particles at the liquid-liquid interface, a new kind of soft material, termed structured liquids, has been put forward. This field emerged from bicontinuous interfacially jammed emulsion gels, or bijels [1, 2], which are prepared by using the spinodal

decomposition of a binary liquid mixture in the presence of the colloidal particles. These particles are trapped at the interface without imposing any preferred interfacial curvature. As phase separation proceeds, the system attempts to reduce the interfacial area, the packing of the particles at the interface densifies, and the particles jam; not allowing the interfacial area to decrease further, phase separation is arrested. And the bicontinuous structure characteristic of spinodal phase separation is locked in [3–6]. However, to obtain stable bijel structure, it usually requires the particles to be strictly neutral wetting at the liquid-liquid interface, which can be a time-consuming and difficult chemical challenge to meet [7]. These disadvantages become increasingly more significant as the size of the particles decreases to the nanoscopic level. Since the size of the particles are small, the binding energy of the particles to the interface is small, and, as a consequence,

the compressive force associated with the reduction in the interfacial area can easily cause the nanoparticles to be ejected from the interface [8, 9]. In addition, the number of fluids that undergo spinodal phase separation is not limitless, and, hence, this rather intriguing behavior becomes less general in applicability.

In this review, we will introduce an alternative strategy to structure liquids by using nanoparticle surfactants (NPSs), where functionalized NPs dispersed in one liquid and polymer/oligomer ligands dissolved in the second liquid interact at the interface between the liquids. The energy holding each NP at the interface can be significantly increased by the self-regulated number of ligands anchored to the NPs. Under

---

\* Shaowei Shi  
shisw@mail.buct.edu.cn

\* Thomas P. Russell  
Russell@mail.pse.umass.edu

<sup>1</sup> Beijing Advanced Innovation Center for Soft Matter Science and Engineering, Beijing University of Chemical Technology, Beijing 100029, China

<sup>2</sup> Department of Polymer Science and Engineering, University of Massachusetts, Amherst, MA 01003, USA

<sup>3</sup> Materials Sciences Division, Lawrence Berkeley National Laboratory, 1 Cyclotron Road, Berkeley, CA 94720, USA

the influence of an external field, such as electric field, jetting, and confinement, liquids can be manipulated to arbitrary shapes, showing promising potential applications in encapsulation, delivery systems, and unique microfluidic devices [9].

## Assembly and jamming of nanoparticles at liquid-liquid interfaces

The thermodynamics of solid particles at the interface was first described by Pieranski [10], by studying the self-assembly of polystyrene spheres at the water-air interface. This theory illuminates that the reducing free energy is the main driving force for the interfacial assembly of particles and also applies to particles at the liquid-liquid interface, e.g., oil-water interface (Fig. 1) [11, 12]. For example, when placing a spherical particle of radius  $r$  from one phase (oil or water) to the interface, the change in the interfacial energy,  $\Delta E$ , can be calculated by the following equation:

$$\Delta E = E - E_{\min} = \frac{1}{4} \pi r^2 (\gamma_{p/o} + \gamma_{p/w} - \gamma_{o/w}) \quad (1)$$

where  $\gamma_{p/o}$ ,  $\gamma_{p/w}$ , and  $\gamma_{o/w}$  are the interfacial tensions of the particle-oil, particle-water, and oil-water interfaces,  $E_{\min}$  is the minimum energy when NP is located at the interface, and  $E_0$  is the energy when NP is located in the oil or water phase. Along with Young's equation,

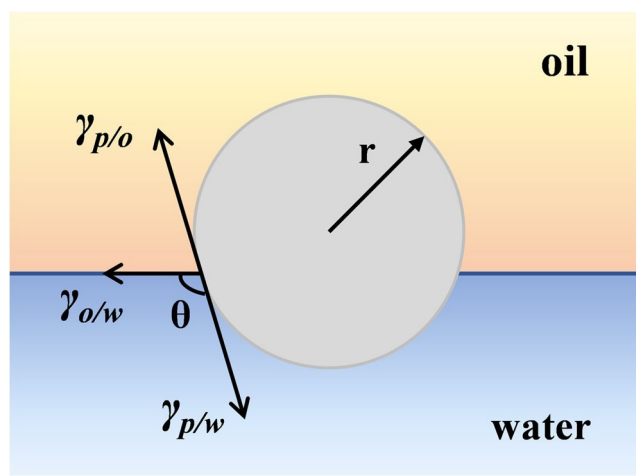
$$\gamma_{p/o} - \gamma_{p/w} = \gamma_{o/w} \cos \theta \quad (2)$$

where

$\theta$  is the contact angle of particles at the interface [9, 12-14] and  $\Delta E$  also can be expressed as

$$\Delta E = \frac{1}{4} \pi r^2 \gamma_{o/w} (1 - \cos \theta) \quad (3)$$

where



From Eqs. 1 and 3, it is clear that, for a given system, the particle stabilization at the oil-water interface is strongly size-dependent. The reduction in the interfacial energy is proportional to the square of the particle radius  $r$ . For micrometer-sized particles, the decrease in total free energy is  $\sim 10^7 k_B T$  ( $k_B$  is the Boltzmann constant,  $T$  is the Kelvin temperature), much larger than thermal energy, leading to an effective confinement of large colloids to the interface [9, 13-18]. However, for nanometer-sized particles, or NPs, the energy reduction is closed to thermal energy (several  $k_B T$ ). As a result, thermal fluctuation can easily detach NPs from the interface, leading to a dynamic or "liquid-like" nature of the assemblies.

As the density of particles at the liquid-liquid interface is increased, the particles will gradually become crowded, forming a particle monolayer in a jammed state at the interface eventually. In this case, the interfacial particles lose mobility and the mechanical properties of the interfacial assemblies are enhanced, showing a "solid-like" nature. More interestingly, the interfacial jamming of particles provides a pathway to shape the liquid-liquid interface in a biphasic system, or in

other words, liquids can be structured to different shapes, just like the solid materials. However, in comparison with micrometer-sized particles, it is difficult to achieve structured liquids using NPs, due to the low interfacial energy of each

Fig. 1 A spherical particle at the oil-water interface

NP. Thus, the NPs can be easily ejected from the interface, unable to maintain the nonequilibrium liquid shapes.

## Nanoparticle surfactants

By dispersing carboxylated polystyrene NPs in water and dissolving amine-terminated polydimethylsiloxane (PDMS- $\text{NH}_2$ ) in oil, Cui et al. developed a method for constructing "Janus-like" nanoparticle surfactants (NPSs) at the oil-water interface [19]. The electrostatic interactions between  $-\text{COO}^-$  and  $-\text{NH}_3^+$  drive the segregation of NPs to the interface, forming a monolayer of NPs. When an electric field was applied, the spherical droplet suspended in oil was deformed into an ellipsoid, exposing more interfacial area, leading to the assembly of more NPSs at the interface. When the electric field was removed, the droplet attempted to return to its spherical shape with the lowest energy (Fig. 2a). However, during the decrease of the interfacial area, NPSs jammed at the interface, arresting the further change of the droplet shape, kinetically trapping the drop into a highly nonequilibrium shape, which can be stable for months (Fig. 2b). The shape of the droplet can be further reconfigured by applying sequential electric fields in the same or different directions, where the NPSs at the interface undergo a local unjamming and jamming process. On the other hand, by using PDMS capped with two amine end groups, the interfacial NPs could be cross-linked, suppressing the deformation of the droplet shape.

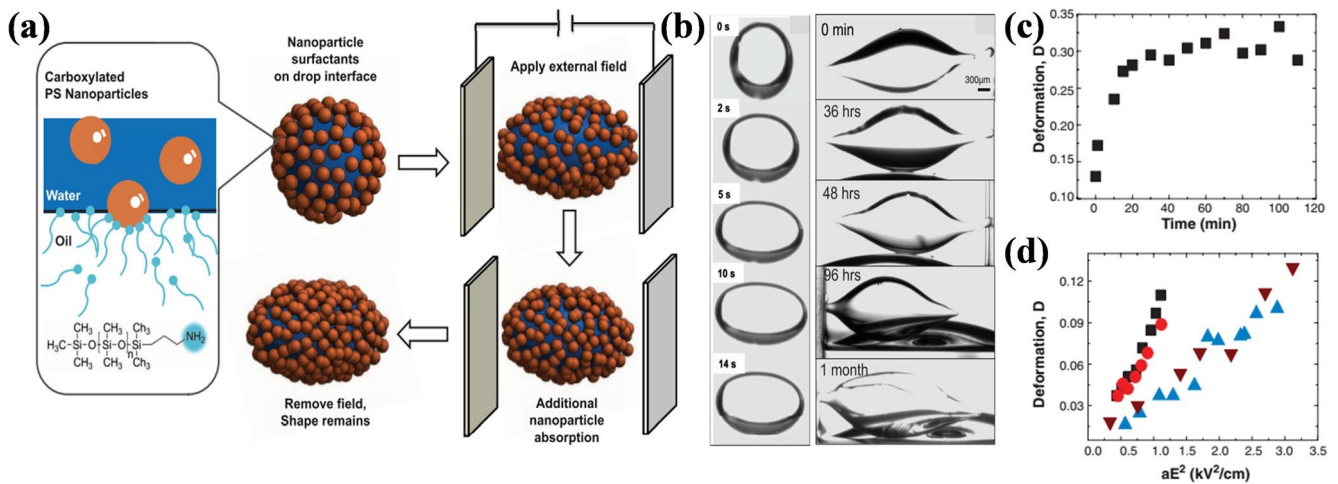


Fig. 2 (a) The schematics of structuring the droplet by an electric field. (b) The deformation and stability of droplets with NPSs assembled at the interface. (c) The deformation of the water droplet with time. (d) The

linear relationship between the  $D$  and  $aE^2$  under various conditions. Reproduced with permission [19]. Copyright 2013, The American Association for the Advancement of Science

The assembly kinetics of NPSs was tracked by investigating the relationship between the deformation ( $D$ ) of the droplet and  $aE^2$  under different conditions, where  $D \approx aE^2/\gamma$ ,  $a$  is the radius of the initial drop,  $E$  is the electric field, and  $\gamma$  is the interfacial tension (Fig. 2d). With only NPs dispersed in aqueous phase against pure oil, the droplet deformation was almost the same as the pure water-oil system. With PDMS-NH<sub>2</sub> dissolved in the oil against pure water, the rate at which  $D$  changed with  $E^2$  increases, indicating that PDMS-NH<sub>2</sub> is a surfactant, and the interfacial tension is decreased. However, when removing the field, the droplet returned to its spherical shape. With NPs dispersed in the aqueous phase and PDMS-NH<sub>2</sub> dissolved in the oil, the rate at which  $D$  changed with  $E^2$  increases further, indicating the formation of the NPSs at the interface and the further reduction in the interfacial tension. These results demonstrate the mechanism of the assembly and formation of the NPSs; that is, the NPs alone are not interfacially active, whereas the PDMS-NH<sub>2</sub> is. As a result, PDMS-NH<sub>2</sub> assembles at the oil-water interface first and then the NPs diffuse to the interface, interacting with PDMS-NH<sub>2</sub>, leading to the formation of the NPSs. The assembly kinetics of NPSs at the water-oil interface can also be probed by tracking the dynamic interfacial tension using pendant drop tensiometry.

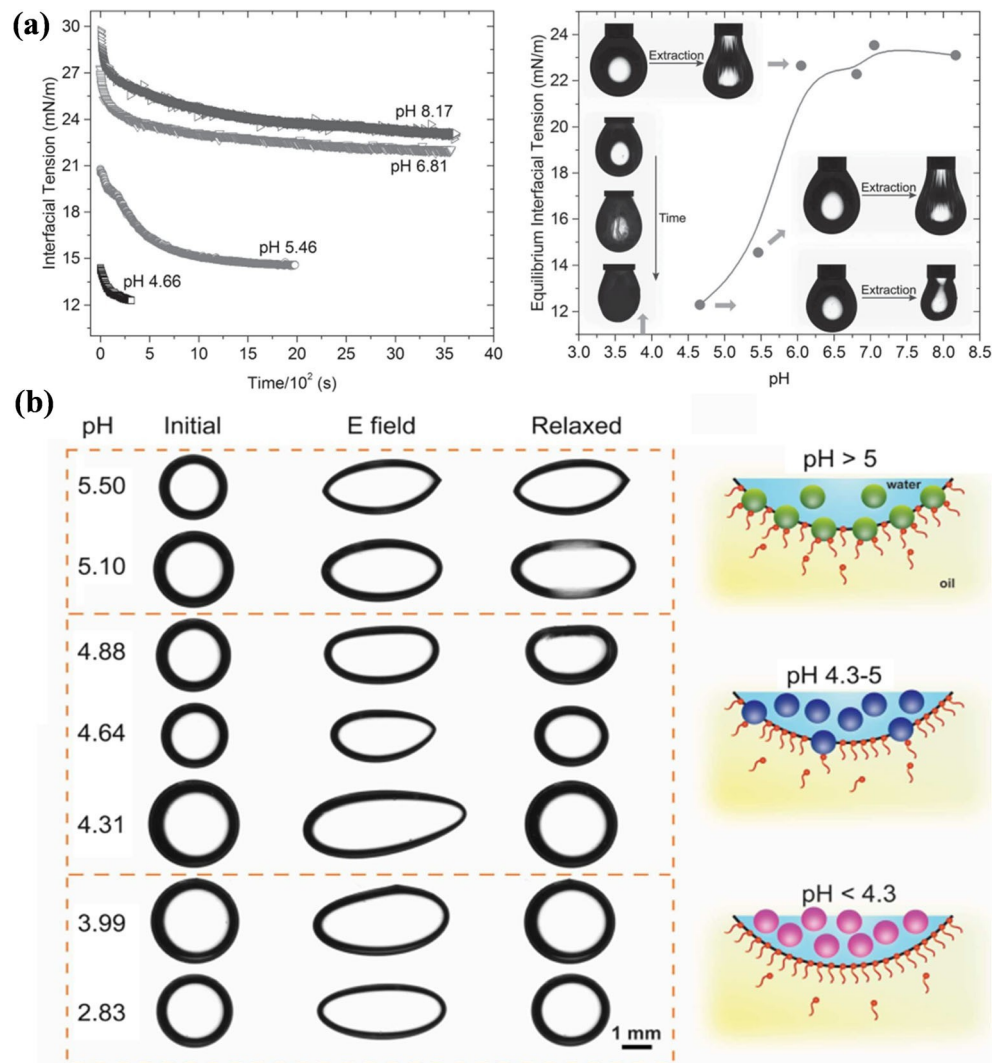
By taking advantage of the cooperative interfacial assembly between NPs and polymer ligands, the interfacial assembly as well as the packing of NPSs can be effectively adjusted by tuning parameters such as the pH, the concentration of NPs/ligands, and the ionic strength of aqueous phase [8, 20]. Huang et al. systematically investigated the effect of pH on the formation and assembly of NPSs, by using carboxylated NPs dispersed in

water and PDMS-NH<sub>2</sub> dissolved in toluene [21]. Since the  $pK_a$  of carboxyl group was  $\sim 4.2$  and the  $pK_a$  of the amine group was  $\sim 9.0$ , in the pH range of 4.2 and 9.0, the deprotonated carboxyl groups and protonated amine groups

interacted strongly at the interface, leading to the formation of the NPSs. The equilibrium interfacial tension decreased with decreasing pH (Fig. 3a). However, it does not mean that at lower pH, more NPSs form at the interface. When the pH was close to the  $pK_a$  of the carboxyl groups, both carboxyl groups and amine groups were highly protonated, and the reduction in the interfacial tension mainly arose from the protonated amine groups. By estimating the interfacial coverage of NPs at different pH and constructing ellipsoidal droplets with an electric field, it showed that when  $pH > 5.0$ , the interfacial coverage of NPs was high and the deformed droplet could be trapped after removing the electric field. In the pH range of 4.3–5.0, the interfacial coverage of NPs decreased and the deformed droplet relaxed to some extent. When the pH was lower than 4.3, the carboxyl groups were almost fully protonated and the electrostatic interactions became weak. The deformed droplet completely returned to spherical shape after removing the electric field (Fig. 3b). By taking advantage of this pH responsiveness, the jamming and unjamming of NPSs at the interface can be reversibly controlled, providing a simple way to reconfigure the structured liquids. After adding base into the water droplet, the droplet could be deformed again with an electric field and maintained in the nonequilibrium shape.

The assembly behavior of NPSs at the oil-water interface can also be controlled by tuning the ionic strength of the aqueous phase. Generally, the charge density of charged particles can be effectively reduced by increasing the ion strength in solution. The electrostatic repulsion between particles can be weakened, leading to an enhanced interfacial activity of particles. This effect is also applicable to NPSs. By increasing the ionic strength of the aqueous phase dispersing carboxylated NPs, Chai et al. obtained a denser packing of NPSs at the oil-water interface and demonstrated the transformation of the interfacial assemblies from liquid-like to solid-like (Fig. 4a)

Fig. 3 (a) pH-Dependent assembly of NPSs at the water-oil interface. (b) Structuring and restructuring liquids through pH-controlled assembly of NPSs. Reproduced with permission [21]. Copyright 2016, Wiley-VCH



[22]. Also, by taking advantage of the in situ AFM, a densely packed state of NPSs at the interface was observed, with crystalline-like arrays in some areas (Fig. 4b).

In general, NPSs provide a simple and universal strategy to realize the stable assembly of NPs at the liquid-liquid interface. The assembled NPs at the interface can be in either



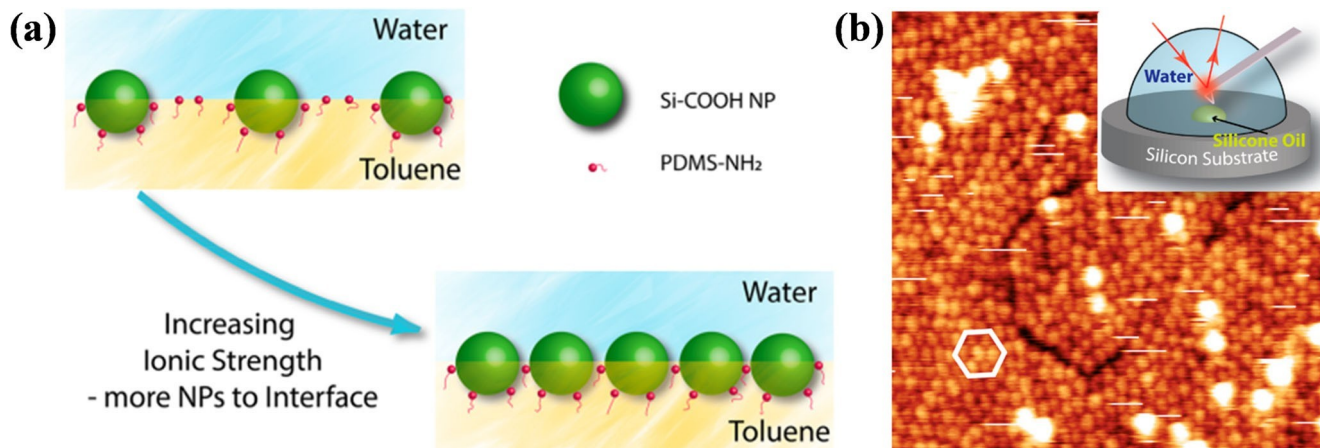


Fig. 4 (a) Schematic diagram of the NPSs assembled at the water-oil interface with increasing ionic strength. (b) In situ AFM image of the interfacial NPS assemblies at 100-mM NaCl. Reproduced with permission [22]. Copyright 2017, American Chemical Society

unjammed or jammed states, which can be readily switched using external triggers such as pH and ionic strength. The mechanical properties of the interfacial assemblies can be effectively tuned by varying the concentration of NPs/ligands, the type of NP/ligand, the NP size, and the ligand molecular weight.

structures could be obtained. In the subsequent work, using a 3D printer, Forth et al. realized the printing of the liquids in high-viscosity silicone oil [28]. Complex liquid devices including sigmoidal and

## Construction of structured liquids

### All-liquid 3D printing

Traditional 3D printing technology is an additive manufacturing process to make solid objects. The 3D printer nozzle is controlled by the computer software to stack molten raw materials layer by layer according to the designed spatial path and finally cool down to make solid parts. The prototype of a 3D-printed object can be derived from a spatial scanning model or electronic data designed by other software, and the 3D object can be processed to any geometric feature [23]. By combining 3D printing with the concept of structured liquids, it would be fascinating if the liquid could be printed using the same design and control methods, which opens a pathway to construct a complex liquid device, where the liquids retain the inherent mobility and transport characteristics yet would permit flow by tailored pathways.

All-liquid 3D printing refers to the technology of printing one liquid with a programmed spatial arrangement in another incompatible liquid phase. To achieve all-liquid 3D printing, an effective suppression of the Plateau-Rayleigh (PR) instabilities of liquid flow is important [24]. In a previous study, the effect of NPSs on PR instabilities was investigated by injecting an aqueous jet dispersed carboxylated NPs into the oil dissolving PDMS-NH<sub>2</sub>. In comparison with the control experiments without NPSs at the interface, longer jet breakup lengths were observed, indicating the significant reduction in the interfacial tension [20, 25, 26]. Later, by using the cooperative assembly of rod-like cellulose nanocrystals (CNCs), and amine-terminated polystyrene (PS-NH<sub>2</sub>), Liu et al. reported the formation and assembly of cellulose nanocrystal surfactants (CNCSs) [27]. The interfacial activity of CNCSs could be significantly enhanced by decreasing the pH, leading to a rapid formation of a CNC monolayer at the interface (Fig. 5a and b). Since jet formation occurs rapidly, this high rate of CNCS formation and assembly is essential to arrest PR instabilities and stabilize the tubular structures. At a certain flow rate, a clear dripping-to-jetting transition was achieved with decreasing pH. By varying parameters such as the concentration of CNC/PS-NH<sub>2</sub>, the flow rate, and the molecular weight of PS-NH<sub>2</sub>, continuous tubular

branched structures were prepared, which could be used for the mass transmission and chemical reactions (Fig. 5c). Further, by using the novel 2D transition metal carbides and nitrides (MXenes) [30–33], Cain et al. presented the creation of all-liquid 3D-printed devices with MXene surfactants, showing potential applications in all-liquid electrochemical and energy storage devices (Fig. 5d) [29].

## All-liquid molding

Similar with 3D printing, the traditional molding method, which is a standard procedure to process polymers in industry, also provides a way of constructing structured liquids. Using the interfacial assembly and jamming of CNCSs, Shi et al. introduce the strategy of all-liquid molding, to produce structured liquids that retain the shape and details of the mold [34]. In this strategy, a 3D printer is used to produce the mold with a patterned trench. The mold is made of hydrophobic polylactic acid (PLA). After prewetting the mold with the PS-NH<sub>2</sub> solution in CCl<sub>4</sub>, an aqueous CNC dispersion is placed into the mold. Without prewetting, the aqueous solution would stick to the corners of the cavity, leading to an unfixed liquid in the trench. After that, the filled mold is immersed into CCl<sub>4</sub> solution dissolving PS-NH<sub>2</sub>, and CNCSs are formed rapidly on the exposed surface. Due to the higher density of CCl<sub>4</sub> than water, the aqueous phase rises out of the mold, with more CNCSs assembled and formed at the interface. In the process of rising, the interface area decreased, leading to a jammed state of CNCSs, arresting further variation of the liquid shape (Fig. 6a).

As we discussed above, pH has significant effects on the interfacial activity of CNCS as well as the structuring of the aqueous phase. As shown in Fig. 6b, with the increase of the pH from 3.0 to 7.0, the fidelity of the molding decreased, and at the pH of 9.0, only spherical droplet could be achieved. Moreover, if the pH was further decreased to 1.2, the CNCs began to aggregate, forming a hydrogel network. Using all-liquid molding, a shaped CNCS-coated gel was prepared with a high fidelity, generating an interfacial bulk gel composite (Fig. 6c).

## Bijels

Huang et al. reported a simple method for preparing bijels by solution shearing at room temperature using NPSs (Fig. 7a) [35]. In this strategy, carboxylated polystyrene NPs were dispersed in water and two different molecular weights of PDMS-NH<sub>2</sub> were dissolved in the oil phase to prepare bijels. By varying the concentration of NPs and polymer ligands, the water/oil ratio, and other factors, the

characteristic size of the bijels could be effectively adjusted, and channel width as low as 500 nm could be achieved (Fig. 7b and c). In comparison with bijels produced via spinodal decomposition, this strategy

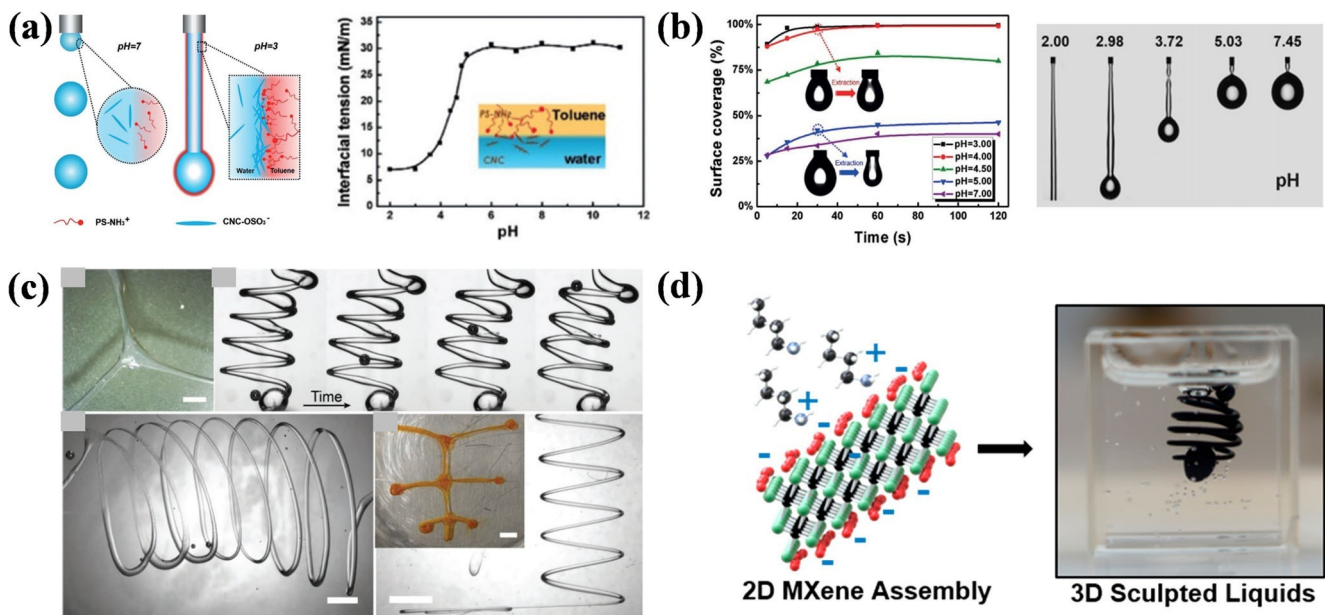
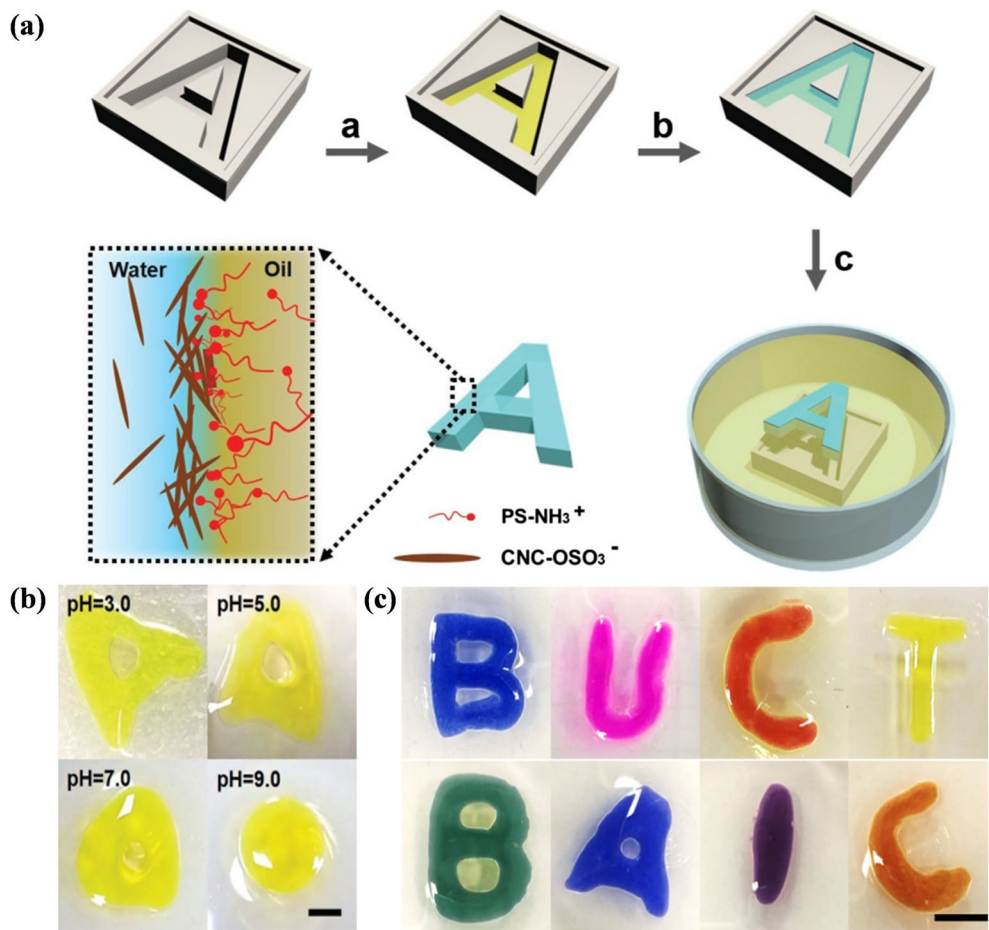


Fig. 5 (a) Schematics of the formation of tubule liquids using CNCs (left) and interfacial activity of CNCs at different pH (right). (b) Surface coverage variation of the droplet with time (left) and breakup length variation of the water jet at different pH (right). Reproduced with permission [27]. Copyright 2017, Wiley-VCH. (c) All-liquid 3D-printed

systems. Reproduced with permission [28]. Copyright 2018, Wiley-VCH. (d) All-liquid 3D-printed devices using MXene surfactants. Reproduced with permission [29]. Copyright 2019, American Chemical Society

Fig. 6 (a) Schematics of all-liquid molding process. (b) Dyed liquid letter molded in different pH. (c) Dyed gel letters molded in pH of 1.2. Scale bar = 5 mm. Reproduced with permission [34]. Copyright 2018, Wiley-VCH





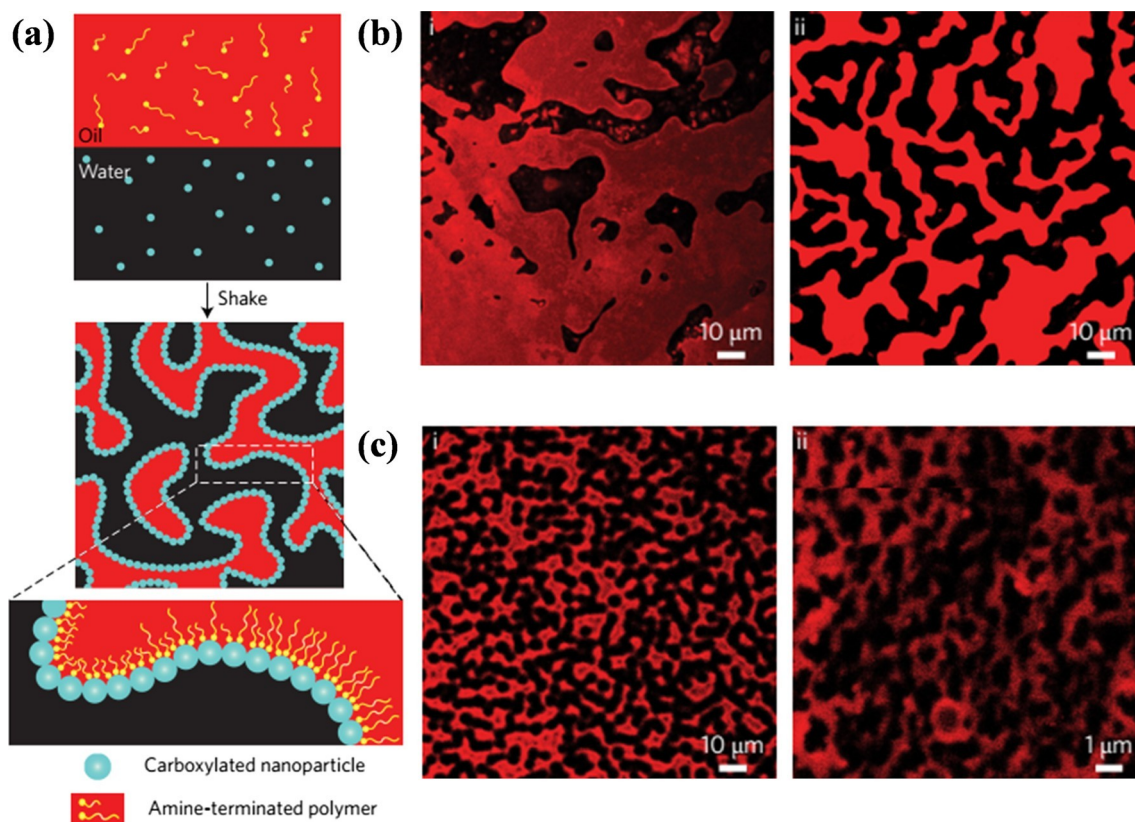


Fig. 7 (a) The preparation of bijels using NPSs at the oil-water interface. (b) Bicontinuous structures formed by NPSs with different NP concentrations at a fixed concentration of PDMS-NH<sub>2</sub>. (c) Bicontinuous

structures formed by NPSs at constant particle concentration with different concentrations of PDMS-NH<sub>2</sub>. Reproduced with permission [35]. Copyright 2017, Springer Nature.

is much easier and universal, which can be used to produce bijel structures using a range of chemistries, where the solvents, particles, and polymer ligands can all be changed.

## Applications

### All-liquid microfluidics

Microfluidics, also known as lab-on-a-chip or microfluidic lab, refers to the technology that processes or manipulates tiny fluids using fluidic channels (tens to hundreds of micrometers in size) [36]. Microfluidics have the ability to miniaturize the basic functions of the laboratory, such as biology and chemistry, onto a few square centimeters chip, and can complete all the steps of sample pretreatment, separation, dilution, mixing, chemical reaction, and detection, so it is also called miniature full-analysis system.

Structured liquids provide a new strategy for the fabrication of all-liquid microfluidic devices. Feng et al. constructed a specific shape of aqueous fluidic channels in the oil phase using nanoclay surfactants and superhydrophobic- superhydrophilic micropatterned

substrates (Fig. 8a) [37]. The fluidic channel based on NPSs is a semipermeable

membrane structure with a negative charge on the hydrophilic side of the surface, which can be used to absorb, transport, and separate substances. When the channel was injected in a mixed aqueous solution dissolving neutral and anionic dye molecules, due to the different affinity of the two dyes in water and oil, the neutral dye molecule could be selectively removed through the walls of the microchannel into the oil phase, and the anionic dye continuously flowed in the channel, which can be collected at the exit, achieving the separation of dye molecules. On the other hand, using the negative charges on the surface of the channel, positively charged dye molecules, biological enzymes, or NPs were successfully adsorbed onto the inner wall of the channel in the process of transmission, endowing the microfluidic devices with functionalities, which can be used as microreactors (Figure 8b and c).

In addition, all-liquid 3D printing can be used to build a “bridge” between independent channels, while the “bridge” can be cut off to restore their independence. The cut channels are self-healing since NPSs can rapidly form and assemble at the interface (Fig. 8d). Based on the characteristics of self-healing and reconfiguration, programmable chemical logic reactors with complex structures can be constructed, and selective transport of reactants in different chemical reactors can be realized by cutting or building bridges between different reactors.

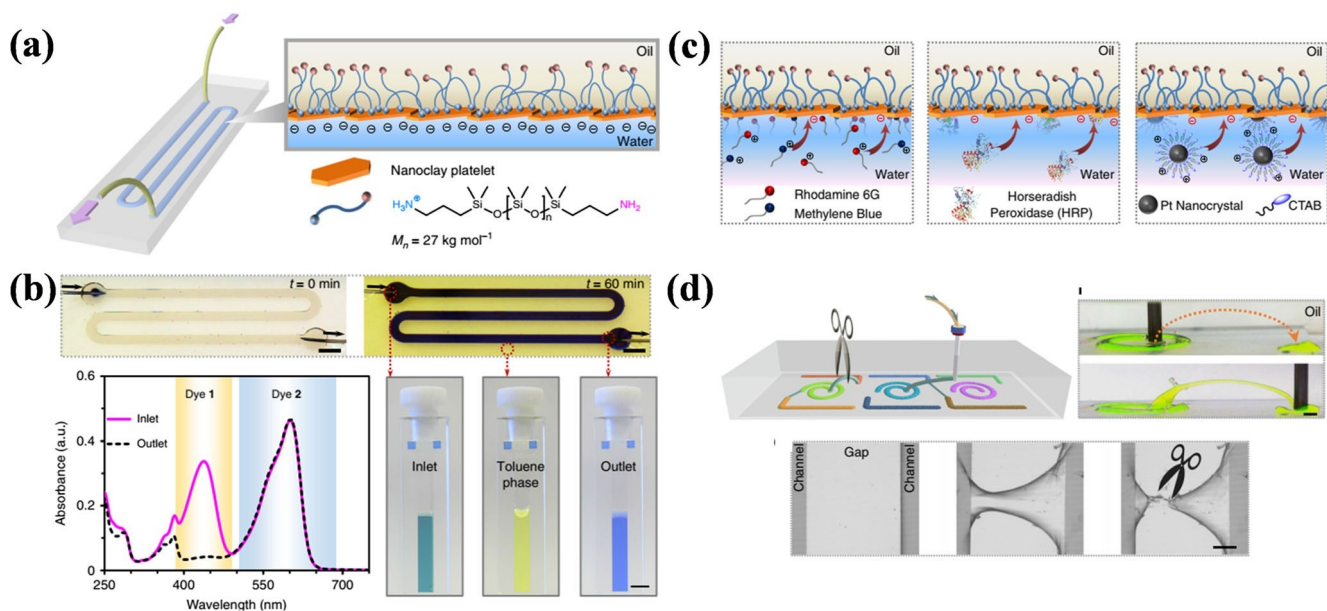


Fig. 8 (a) Schematics of all-liquid microfluidic devices. (b) Mass separation of different dye molecules in fluidic channels. (c) The functionalization of the anionic NPS film using cationic molecules,

enzymes, and nanocrystals. (d) Reconfiguration and self-healing of all-liquid microfluidic devices. Reproduced with permission [37]. Copyright 2019, Springer Nature

## Pickering emulsions and polymer nanocomposites

NPS also provides an easy way to fabricate Pickering emulsions with functionalities [38–42]. Using carboxylated silica NPs or polystyrene NPs dispersed in aqueous phase and oil-soluble polymer ligands such as PDMS-NH<sub>2</sub>, NH<sub>2</sub>-PDMS-NH<sub>2</sub>, or poly[dimethylsiloxane-co-(3-aminopropyl)methylsiloxane] copolymer, Toor et al. successfully produced NPS-stabilized aqueous droplets using a microfluidic device (Figure 9a and b) [43]. The mechanical properties of the interfacial assemblies can be effectively manipulated by using different types of polymer ligands or varying the molecular weight of polymer ligands. Due to the presence of NPS layer at the interface, the coalescence of the droplet can be arrested, preventing the exchange of materials across interfaces. NPs, dyes, and proteins with diameters in the 2.4 – 30 nm range can be encapsulated successfully (Fig. 9c, d, and e).

By mechanically shearing the suspension of CNC in the water phase and PS-NH<sub>2</sub> in the toluene phase, Li et al. prepared o/w Pickering emulsions stabilized by CNCs (Figure 10a) [44]. By varying pH, the size and morphology of the emulsions can be effectively manipulated. It is interesting that at a low pH, structured emulsions could be prepared, due to the interfacial jamming of the CNCs during homogenization. No structured emulsions were achieved at higher pH, indicating the loose packing of CNCs at the interface. Using the concentrated emulsions

stabilized by CNCs as templates, a dry CNC/PS composite foam was fabricated by freeze-drying. The pore size and shape of the foam cell could be effectively controlled, which were commensurate with the emulsion droplets (Fig.10b). Also, the prepared foam was

responsive to pH, which could keep its stability in the acid environment and be destroyed in the basic environment.

This strategy can be used for a broad range of nanomaterials. In the subsequent study, Shi et al. used MXene ( $\text{Ti}_3\text{C}_2\text{T}_x$ ) and amine-functionalized polyhedral oligo-silsesquioxane (POSS-NH<sub>2</sub>) to form MXene surfactants (MXSs) at the oil-water interface [45]. Stable w/o Pickering emulsions could be easily prepared using MXSs, and lightweight MXene aerogels with excellent mechanical properties could be achieved (Fig. 10c, d, and e). The as-prepared MXene aerogels showed excellent oil absorbency, and the fabricated MXene/epoxy nanocomposites showed good performance in the EMI shielding (Fig. 10f and g).

## Ferromagnetic liquid droplets

When magnetic nanoparticles (MNPs) are dispersed in carrier fluids, paramagnetic ferrofluids are formed [46–50]. On the other hand, if the Brownian motion of the MNPs is suppressed, the transformation of a ferrofluid into a ferromagnetic material can be achieved [51]. Recently, by taking advantage of the jamming of MNP surfactants (MNPSs) at the oil-water interface, Liu et al. reported a simple strategy to realize a paramagnetism to ferromagnetism transformation at room temperature [52]. In this study, they used an aqueous dispersion of carboxylated MNPs ( $\text{Fe}_3\text{O}_4\text{-COOH}$ ) and a solution of POSS-NH<sub>2</sub> in oil to form MNPSs at the oil-water interface. When the MNPSs jam at the interface, the ferrofluid droplet transforms into a ferromagnetic liquid droplet, which is confirmed by the magnetic hysteresis loops (Fig. 11a). By combining all-liquid 3D printing with microfluidic technology, ferromagnetic liquid cylinders were



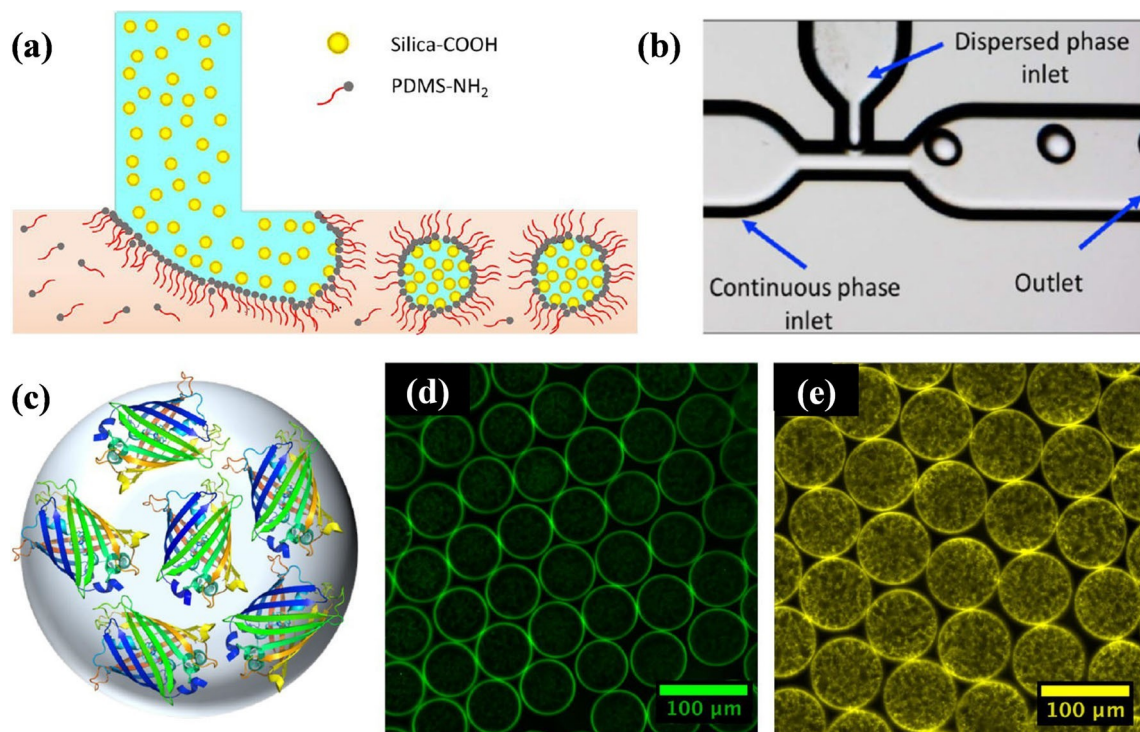


Fig. 9 (a, b) Schematics of the formation of w/o droplets in a microfluidic T-junction. (c) Schematic of an NPS-stabilized water droplet containing fluorescent proteins. (d, e) Confocal laser scanning microscopy images

showing encapsulation of enhanced green fluorescent protein and yellow fluorescent protein. Reproduced with permission [43]. Copyright 2018, American Chemical Society

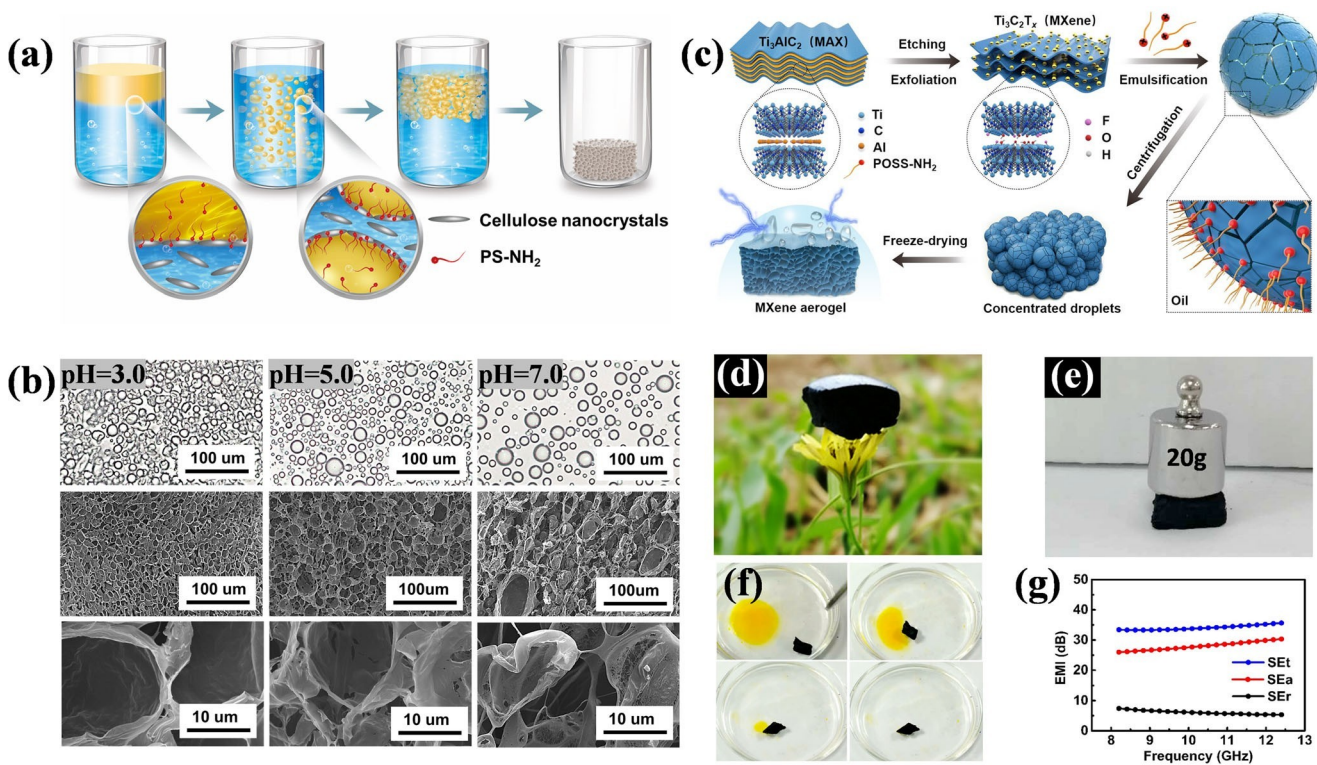


Fig.10 (a) Schematics of the preparation of the CNCS-based emulsions and foams. (b) Optical micrographs of Pickering emulsion droplets stabilized by CNCSs at different pH. Reproduced with permission [44]. Copyright 2018, Wiley-VCH. (c) Schematic showing the construction of Pickering emulsions and MXene

aerogels via MXSs. (d, e) A small

piece of MXene aerogel on a flower and a small piece of aerogel (~6.4 mg) supporting a 20-g weight. (f, g) Oil absorption of MXene aerogel and EMI shielding performance of MXene/epoxy nanocomposite. Reproduced with permission [45]. Copyright 2019, Wiley-VCH

produced. In a magnetic field gradient generated by the aluminum solenoid, a liquid cylinder was magnetized and pulled into the solenoid (Fig. 11b). The magnetized liquid cylinders behave like solid magnets, and N-N, S-S, and N-S dipole interactions can be obtained (Fig. 11c).

The prepared ferromagnetic liquid droplets show both the fluid characteristics of liquids and the magnetic properties of solids, with excellent reconfiguration (Fig. 11d and e). Taking advantage of these intriguing properties, separation and patterning of ferromagnetic liquid droplets could be easily achieved. As shown in Fig. 11f and g, in comparison with the ferrofluid droplets, the ferromagnetic liquid droplets were attracted much more strongly to a static bar magnet and could rotate when using a rotating magnet.

## Photoresponsive structured liquids

As discussed above, the assembly and formation of NPSs mainly depend on electrostatic interactions between ion pairs (e.g.,  $-\text{COO}^-$  and  $\text{NH}_3^+$ ), and only pH responsiveness of the interfacial assemblies can be obtained, which limits the construction of structured liquids with complex multiple responsiveness. Recently Sun et al. reported the construction of photoresponsive NPSs as well as structured liquids using the host-guest interactions between  $\alpha$ -cyclodextrin ( $\alpha$ -CD) and azobenzene (Azo) at the oil-water interface (Fig. 12a) [53]. In this system,  $\alpha$ -CD-

modified gold NP with low interfacial activity was dispersed in water and Azo-terminated poly-L-lactide (Azo-PLLA) were dissolved in toluene. NPSs were formed in situ at the interface. It should be noted that Azo-PLLA behaves like a surfactant. The carbonyl groups in Azo-PLLA could hydrogen bond with water, locating the terminal Azo groups at the interface, which played an important role in triggering the molecular recognition of  $\alpha$ -CD and Azo at the interface (Fig. 12b). 2D films can be easily prepared at the oil-water interface and TEM image shows a monolayer of close-packed Au-NPs (Fig. 12c).

The photoresponsiveness of the NPSs was investigated by using a wrinkled droplet, where the NPSs were in a jammed state. No change of the droplet shape was observed under visible light. However, under ultraviolet (UV) irradiation, the wrinkled droplet gradually relaxed and returned to a spherical shape, indicating the jamming-to-unjamming transformation of the NPSs. This transformation is reversible and the NPSs could be re-jammed when UV irradiation was stopped (Fig. 12d).

## Summary and prospect

NPSs provide a new strategy for the design and construction of complex structured liquids. This review mainly summarizes the formation mechanism of NPSs, the construction of structured liquids, and applications. The assembly and packing behavior of NPs at the interface can be effectively manipulated by

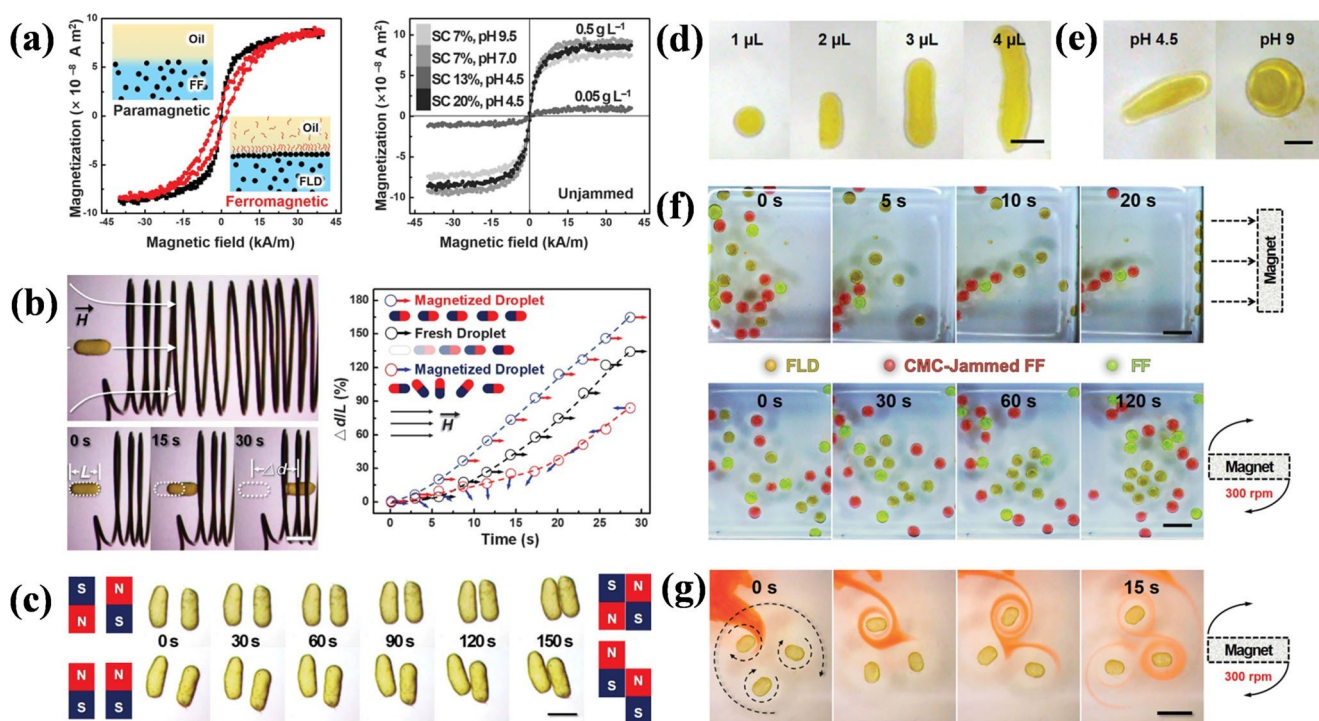


**Fig. 11** (a) Magnetic hysteresis loops of droplets with and without jammed MNPSs at the interface. (b) The motion of a magnetized liquid cylinder in a magnetic field gradient, generated by the aluminum solenoid. (c) Dipole interaction between two magnetized liquid cylinders. (d)

Droplets of different aspect ratios. (e) Reconfiguration of the droplet by tuning the pH. (f and g) Sorting FLDs by using static and rotational magnetic fields. Reproduced with permission [52]. Copyright 2019, The American Association for the Advancement of Science.



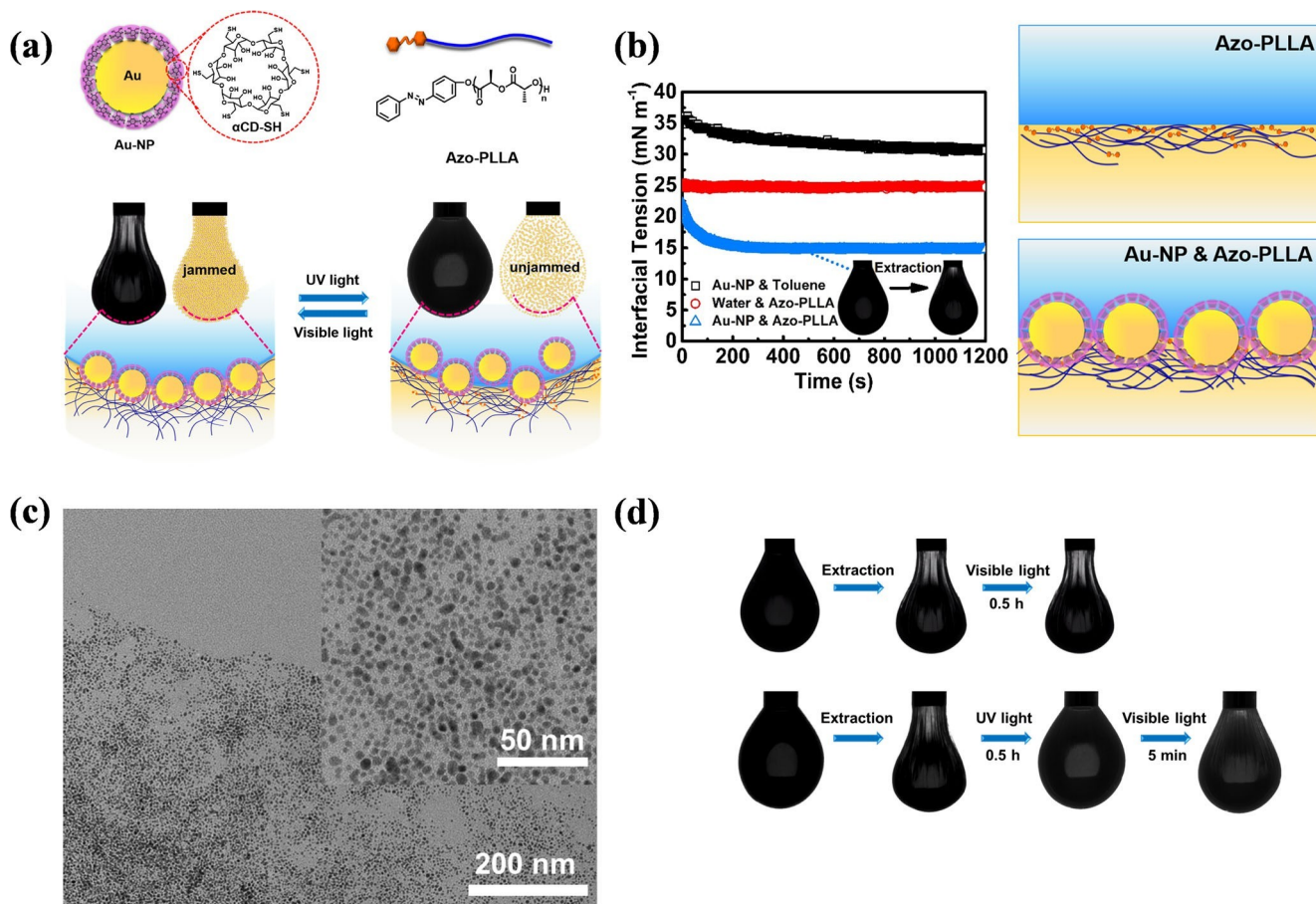


Fig. 12 (a) Schematics of the photoresponsive NPSs at the oil-water interface. (b) Assembly kinetics of the photoresponsive NPSs at the oil-water interface. (c) TEM image of 2D films assembled at the interface. (d)

Photosensitivity of the wrinkled droplet. Reproduced with permission [53]. Copyright 2020, American Chemical Society

adjusting the two parts of NPS (NP and polymer/oligomer ligand). Using external field and jammed NPSs at the interface, liquids can be printed or molded to desired shapes, just like solid materials, with responsiveness to the environment.

There is much we do not understand with this behavior and the field is wide open for further exploration. NPs such as carbon nanotube, graphene oxide, fullerene, and polyoxometalate can be used to construct functional assemblies including colloidosome, 2D nanofilms, polymer nanocomposites and structured liquids [20, 25, 29, 54, 55]. The concept of NPSs can be further extended to other systems without NPs, such as polyelectrolyte and even small molecule systems. For example, recently we obtained a fibrous supramolecular structure at the oil-water interface using water-soluble porphyrins assembled with polymer ligands [56]. Also, by using the cooperative assembly of polyelectrolyte and ligands, we put forward the concept of polyelectrolyte surfactants (PESs) [57, 58]. On the other hand, different liquid systems, e.g., aqueous two-phase system and oil/oil system, can

be used to construct structured liquids [59–62]. The generation of multiple stimuli-responsive structured liquids is an emerging field just started, which can be achieved

either by exploring new interactions at the interface [56, 63–65] or synthesizing NPs and functional polymer/oligomer ligands [66–70].

Funding T.P.R. was supported by the US Department of Energy, Office of Science, Office of Basic Energy Sciences, Materials Sciences and Engineering Division under Contract No. DE-AC02-05-CH11231 within the Adaptive Inter-facial Assemblies Towards Structuring Liquids program (KCTR16). This work was supported by the Beijing Natural Science Foundation (2194083) and National Natural Science Foundation of China (51903011).

## Compliance with ethical standards

Conflict of interest The authors declare that they have no conflict of interest

## References

1. Stratford K, Adhikari R, Pagonabarraga I, Desplat JC, Cates ME (2005) Colloidal jamming at interfaces: a route to fluid-bicontinuous gels. *Science* 309(5744):2198–2201. <https://doi.org/10.1126/science.1116589>

2. Herzig EM, White KA, Schofield AB, Poon WCK, Clegg PS (2007) Bicontinuous emulsions stabilized solely by colloidal particles. *Nature Mater* 6(12):966–971. <https://doi.org/10.1038/nmat2055>
3. Lee MN, Mohraz A (2010) Bicontinuous macroporous materials from bijel templates. *Adv Mater* 22(43):4836–4841. <https://doi.org/10.1002/adma.201001696>
4. Lee MN, Mohraz A (2011) Hierarchically porous silver monoliths from colloidal bicontinuous interfacially jammed emulsion gels. *J Am Chem Soc* 133(18):6945–6947. <https://doi.org/10.1021/ja201650z>
5. Lee MN, Thijssen JHJ, Witt JA, Clegg PS, Mohraz A (2013) Making a robust interfacial scaffold: bijel rheology and its link to processability. *Adv Funct Mater* 23(4):417–423. <https://doi.org/10.1002/adfm.201201090>
6. Hijnen N, Cai D, Clegg PS (2015) Bijels stabilized using rod-like particles. *Soft Matter* 11(22):4351–4355. <https://doi.org/10.1039/C5SM00265F>
7. Mohraz A (2017) Simple shaking yields bicontinuity. *Nature Nanotech* 12(11):1021–1022. <https://doi.org/10.1038/nnano.2017.201>
8. Shi S, Russell TP (2018) Nanoparticle assembly at liquid-liquid interfaces: from the nanoscale to mesoscale. *Adv Mater* 30(44):1800714. <https://doi.org/10.1002/adma.201800714>
9. Forth J, Kim PY, Xie G, Liu X, Helms BA, Russell TP (2019) Building reconfigurable devices using complex liquid-fluid interfaces. *Adv Mater* 31(18):e1806370. <https://doi.org/10.1002/adma.201806370>
10. Pieranski P (1980) Two-dimensional interfacial colloidal crystals. *Phys Rev Lett* 45(7):569–572. <https://doi.org/10.1103/PhysRevLett.45.569>
11. Dong L, Johnson D (2003) Surface tension of charge-stabilized colloidal suspensions at the water-air interface. *Langmuir* 19(24):10205–10209. <https://doi.org/10.1021/la035128j>
12. Bernard PB, John HC (2002) Solid wettability from surface energy components: relevance to Pickering emulsions. *Langmuir* 18(4):1270–1273. <https://doi.org/10.1021/la011420k>
13. Booth SG, Dryfe RAW (2015) Assembly of nanoscale objects at the liquid/liquid interface. *J Phys Chem C* 119(41):23295–23309. <https://doi.org/10.1021/acs.jpcc.5b07733>
14. Maestro A, Guzmán E, Ortega F, Rubio RG (2014) Contact angle of micro- and nanoparticles at fluid interfaces. *Curr Opin Colloid Interface Sci* 19(4):355–367. <https://doi.org/10.1016/j.cocis.2014.04.008>
15. Binks BP, Lumsdon SO (2000) Influence of particle wettability on the type and stability of surfactant-free emulsions. *Langmuir* 16(23):8622–8631. <https://doi.org/10.1021/la000189s>
16. Binks BP, Clint JH (2002) Solid wettability from surface energy components: relevance to Pickering emulsions. *Langmuir* 18(4):1270–1273. <https://doi.org/10.1021/la011420k>
17. Santini E, Guzmán E, Ravera F, Ferrari M, Liggieri L (2012) Properties and structure of interfacial layers formed by hydrophilic silica dispersions and palmitic acid. *Phys Chem Chem Phys* 14(2):607–615. <https://doi.org/10.1039/C1CP22552A>
18. Santini E, Guzmán E, Ferrari M, Liggieri L (2014) Emulsions stabilized by the interaction of silica nanoparticles and palmitic acid at the water–hexane interface. *Colloids Surf A Physicochem Eng Aspects* 460:333–341. <https://doi.org/10.1016/j.colsurfa.2014.02.054>
19. Cui M, Emrick T, Russell TP (2013) Stabilizing liquid drops in nonequilibrium shapes by the interfacial jamming of nanoparticles. *Science* 342(6157):460–463. <https://doi.org/10.1126/science.1242852>
20. Sun Z, Feng T, Russell TP (2013) Assembly of graphene oxide at water/oil interfaces: tessellated nanotiles. *Langmuir*

21. Huang C, Sun Z, Cui M, Liu F, Helms BA, Russell TP (2016) Structured liquids with pH-triggered reconfigurability. *Adv Mater* 28(31):6612–6618. <https://doi.org/10.1002/adma.201600691>
22. Chai Y, Lukito A, Jiang Y, Ashby PD, Russell TP (2017) Fine-tuning nanoparticle packing at water-oil interfaces using ionic strength. *Nano Lett* 17(10):6453–6457. <https://doi.org/10.1021/acs.nanolett.7b03462>
23. Ngo TD, Kashani A, Imbalzano G, Nguyen KTQ, Hui D (2018) Additive manufacturing (3D printing): a review of materials, methods, applications and challenges. *Compos Part B-Eng* 143: 172–196. <https://doi.org/10.1016/j.compositesb.2018.02.012>
24. Mead-Hunter R, King AJ, Mullins BJ (2012) Plateau Rayleigh instability simulation. *Langmuir* 28(17):6731–6735. <https://doi.org/10.1021/la300622h>
25. Feng T, Hoagland DA, Russell TP (2014) Assembly of acid-functionalized single-walled carbon nanotubes at oil/water interfaces. *Langmuir* 30(4):1072–1079. <https://doi.org/10.1021/la404543s>
26. Toor A, Helms BA, Russell TP (2017) Effect of nanoparticle surfactants on the breakup of free-falling water jets during continuous processing of reconfigurable structured liquid droplets. *Nano Lett* 17(5):3119–3125. <https://doi.org/10.1021/acs.nanolett.7b00556>
27. Liu X, Shi S, Li Y, Joe F, Wang D, Russell TP (2017) Liquid tubule formation and stabilization using cellulose nanocrystal surfactants. *Angew Chem Int Ed* 56(41):12594–12598. <https://doi.org/10.1002/anie.201706839>
28. Forth J, Liu X, Hasnain J, Toor A, Miszta K, Shi S, Geissler PL, Emrick T, Helms BA, Russell TP (2018) Reconfigurable printed liquids. *Adv Mater* 30(16):1707603. <https://doi.org/10.1002/adma.201707603>
29. Cain JD, Azizi A, Maleski K, Anasori B, Glazer EC, Kim PY, Gogotsi Y, Helms BA, Russell TP, Zettl A (2019) Sculpting liquids with two-dimensional materials: the assembly of Ti<sub>3</sub>C<sub>2</sub>T<sub>x</sub> MXene sheets at liquid-liquid interfaces. *ACS Nano* 13(11):12385–12392. <https://doi.org/10.1021/acsnano.9b05088>
30. Naguib M, Kurtoglu M, Presser V, Lu J, Niu J, Heon M, Hultman L, Gogotsi Y, Barsoum MW (2011) Two-dimensional nanocrystals produced by exfoliation of Ti<sub>3</sub>AlC<sub>2</sub>. *Adv Mater* 23(37):4248–4253. <https://doi.org/10.1002/adma.201102306>
31. Naguib M, Mochalin VN, Barsoum MW, Gogotsi Y (2014) 25th anniversary article: MXenes: a new family of two-dimensional materials. *Adv Mater* 26(7):992–1005. <https://doi.org/10.1002/adma.201304138>
32. Liu J, Zhang HB, Sun R, Liu Y, Liu Z, Zhou A, Yu ZZ (2017) Hydrophobic, flexible, and lightweight MXene foams for high-performance electromagnetic-interference shielding. *Adv Mater* 29(38):1702367. <https://doi.org/10.1002/adma.201702367>
33. Bian R, Lin R, Wang G, Lu G, Zhi W, Xiang S, Wang T, Clegg PS, Cai D, Huang W (2018) 3D assembly of Ti<sub>3</sub>C<sub>2</sub>-MXene directed by water/oil interfaces. *Nanoscale* 10(8):3621–3625. <https://doi.org/10.1039/c7nr07346a>
34. Shi S, Liu X, Li Y, Wu X, Wang D, Forth J, Russell TP (2018) Liquid letters. *Adv Mater* 30(9):1705800. <https://doi.org/10.1002/adma.201705800>
35. Huang C, Forth J, Wang W, Hong K, Smith GS, Helms BA, Russell TP (2017) Bicontinuous structured liquids with sub-micrometre domains using nanoparticle surfactants. *Nature Nanotech* 12(11): 1060–1063. <https://doi.org/10.1038/nnano.2017.182>
36. Mark D, Haerberle S, Roth G, Von Stetten F, Zengerle R (2010) Microfluidic lab-on-a-chip platforms: requirements, characteristics and applications. In: *Microfluidics based microsystems*. Springer, pp 305–376
37. Feng W, Chai Y, Forth J, Ashby PD, Russell TP, Helms BA (2019) Harnessing liquid-in-liquid printing and micropatterned substrates to fabricate 3-dimensional all-liquid fluidic devices. *Nat Commun* 10(1):1095. <https://doi.org/10.1038/s41467-019-09042-y>

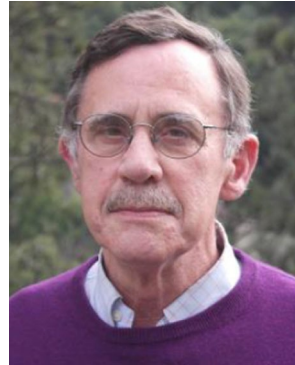


38. Pickering SU (1907) CXCVI.—Emulsions. *Journal of the Chemical Society, Transactions* 91:2001–2021. <https://doi.org/10.1039/CT9079102001>
39. Ramsden W, Gotch F (1904) Separation of solids in the surface-layers of solutions and ‘suspensions’ (observations on surface-membranes, bubbles, emulsions, and mechanical coagulation). — Preliminary account. *Proc R Soc London* 72(477-486):156–164. <https://doi.org/10.1098/rspl.1903.0034>
40. Chevalier Y, Bolzinger M-A (2013) Emulsions stabilized with solid nanoparticles: Pickering emulsions. *Colloids Surf A: Physicochemical and Engineering Aspects* 439:23–34. <https://doi.org/10.1016/j.colsurfa.2013.02.054>
41. Yang Y, Fang Z, Chen X, Zhang W, Xie Y, Chen Y, Liu Z, Yuan W (2017) An overview of Pickering emulsions: solid-particle materials, classification, morphology, and applications. *Front Pharmacol* 8(287). <https://doi.org/10.3389/fphar.2017.00287>
42. Chen T, Colver PJ, Bon SAF (2007) Organic–inorganic hybrid hollow spheres prepared from TiO<sub>2</sub>-stabilized Pickering emulsion polymerization. *Adv Mater* 19(17):2286–2289. <https://doi.org/10.1002/adma.200602447>
43. Toor A, Lamb S, Helms BA, Russell TP (2018) Reconfigurable microfluidic droplets stabilized by nanoparticle surfactants. *ACS Nano* 12(3):2365–2372. <https://doi.org/10.1021/acs.nano.7b07635>
44. Li Y, Liu X, Zhang Z, Zhao S, Tian G, Zheng J, Wang D, Shi S, Russell TP (2018) Adaptive structured Pickering emulsions and porous materials based on cellulose nanocrystal surfactants. *Angew Chem Int Ed* 57(41):13560–13564. <https://doi.org/10.1002/anie.201808888>
45. Shi S, Qian B, Wu X, Sun H, Wang H, Zhang HB, Yu ZZ, Russell TP (2019) Self-assembly of MXene-surfactants at liquid-liquid interfaces: from structured liquids to 3D aerogels. *Angew Chem Int Ed* 58(50):18171–18176. <https://doi.org/10.1002/anie.201908402>
46. Shliomis MI (1974) Magnetic fluids. *Soviet Physics Uspekhi* 17(2): 153–169. <https://doi.org/10.1070/pu1974v017n02abeh004332>
47. Blums E, Cebers A, Maiorov MM (2010) *Magnetic fluids*. Walter de Gruyter
48. Berkovski B, Bashtovoy V (1996) *Magnetic fluids and applications handbook*, vol 36. Begell House, New York
49. Massart R, Dubois E, Cabuil V, Hasmonay E (1995) Preparation and properties of monodisperse magnetic fluids. *J Magn Mater* 149(1-2):1–5. [https://doi.org/10.1016/0304-8853\(95\)00316-9](https://doi.org/10.1016/0304-8853(95)00316-9)
50. Pileni MP (2001) Magnetic fluids: fabrication, magnetic properties, and organization of nanocrystals. *Adv Funct Mater* 11(5):323–336. [https://doi.org/10.1002/1616-3028\(200110\)11:53.0.CO;2-J](https://doi.org/10.1002/1616-3028(200110)11:53.0.CO;2-J)
51. Rosensweig RE (2013) *Ferrohydrodynamics*. Courier Corporation
52. Liu X, Kent N, Ceballos A, Streubel R, Jiang Y, Chai Y, Kim PY, Forth J, Hellman F, Shi S (2019) Reconfigurable ferromagnetic liquid droplets. *Science* 365(6450):264–267. <https://doi.org/10.1126/science.aaw8719>
53. Sun H, Li L, Russell TP, Shi S (2020) Photoresponsive structured liquids enabled by molecular recognition at liquid-liquid interfaces. *J Am Chem Soc.* 142:8591–8595. <https://doi.org/10.1021/jacs.0c02555>
54. Li R, Chai Y, Jiang Y, Ashby PD, Toor A, Russell TP (2017) Carboxylated fullerene at the oil/water interface. *ACS Appl Mater Interfaces* 9(39):34389–34395. <https://doi.org/10.1021/acsami.7b07154>
55. Huang C, Chai Y, Jiang Y, Forth J, Ashby PD, Arras MML, Hong K, Smith GS, Yin P, Russell TP (2018) The interfacial assembly of polyoxometalate nanoparticle surfactants. *Nano Lett* 18(4):2525–2529. <https://doi.org/10.1021/acs.nanolett.8b00208>
56. Gu PY, Chai Y, Hou H, Xie G, Jiang Y, Xu QF, Liu F, Ashby PD, Lu JM, Russell TP (2019) Stabilizing liquids using interfacial supramolecular polymerization. *Angew Chem Int Ed* 58(35):12112–12116. <https://doi.org/10.1002/anie.201906339>

57. Qian B, Shi S, Wang H, Russell TP (2020) Reconfigurable liquids stabilized by DNA surfactants. *ACS Appl Mater Interfaces* 12(11): 13551–13557. <https://doi.org/10.1021/acsami.0c01487>
58. Xu R, Liu T, Sun H, Wang B, Shi S, Russell TP (2020) Interfacial assembly and jamming of polyelectrolyte surfactants: a simple route to print liquids in low-viscosity solution. *ACS Appl Mater Interfaces* 12(15):18116–18122. <https://doi.org/10.1021/acsami.0c00577>
59. Luo G, Yu Y, Yuan Y, Chen X, Liu Z, Kong T (2019) Freeform, reconfigurable embedded printing of all-aqueous 3D architectures. *Adv Mater* 31(49):1904631. <https://doi.org/10.1002/adma.201904631>
60. Hann SD, Lee D, Stebe KJ (2017) Tuning interfacial complexation in aqueous two phase systems with polyelectrolytes and nanoparticles for compound all water emulsion bodies (AWE-somes). *Phys Chem Chem Phys* 19(35):23825–23831. <https://doi.org/10.1039/C7CP02809A>
61. Hann SD, Stebe KJ, Lee D (2017) AWE-somes: all water emulsion bodies with permeable shells and selective compartments. *ACS Appl Mater Interfaces* 9(29):25023–25028. <https://doi.org/10.1021/acsami.7b05800>
62. Xie G, Forth J, Zhu S, Helms BA, Ashby PD, Shum HC, Russell TP (2020) Hanging droplets from liquid surfaces. *Proc Natl Acad Sci USA* 117(15):8360–8365. <https://doi.org/10.1073/pnas.1922045117>
63. Zhang J, Coulston RJ, Jones ST, Geng J, Scherman OA, Abell C (2012) One-step fabrication of supramolecular microcapsules from microfluidic droplets. *Science* 335(6069):690–694. <https://doi.org/10.1126/science.1215416>
64. Zheng Y, Yu Z, Parker RM, Wu Y, Abell C, Scherman OA (2014) Interfacial assembly of dendritic microcapsules with host-guest chemistry. *Nat Commun* 5:5772. <https://doi.org/10.1038/ncomms6772>
65. Patra D, Ozdemir F, Miranda O, Samanta B, Sanyal A, Rotello V (2009) Formation and size tuning of colloidal microcapsules via host-guest molecular recognition at the liquid-liquid interface. *Langmuir* 25:13852–13854. <https://doi.org/10.1021/la9015756>
66. Luo J, Zeng M, Peng B, Tang Y, Zhang L, Wang P, He L, Huang D, Wang L, Wang X, Chen M, Lei S, Lin P, Chen Y, Cheng Z (2018) Electrostatic-driven dynamic jamming of 2D nanoparticles at interfaces for controlled molecular diffusion. *Angew Chem Int Ed* 130(36):11926–11931. <https://doi.org/10.1002/ange.201807372>
67. Jiang Y, Chakroun R, Groschel AH, Russell TP (2020) Soft polymer Janus nanoparticles at liquid/liquid interfaces. *Angew Chem Int Ed*. 59:12751–12755. <https://doi.org/10.1002/anie.202004162>
68. Gao Y, Zhao CX, Sainsbury F (2020) Droplet shape control using microfluidics and designer biosurfactants. <https://doi.org/10.26434/chemrxiv.12103284>
69. Yang Z, Wei J, Sobolev YI, Grzybowski BA (2018) Systems of mechanized and reactive droplets powered by multi-responsive surfactants. *Nature* 553(7688):313–318. <https://doi.org/10.1038/nature25137>
70. Hou H, Li J, Li X, Forth J, Yin J, Jiang X, Helms BA, Russell TP (2019) Interfacial activity of amine-functionalized polyhedral oligomeric silsesquioxanes (POSS): a simple strategy to structure liquids. *Angew Chem Int Ed* 131(30):10248–10253. <https://doi.org/10.1002/anie.201903420>



Shaowei Shi received his B.S. (2010) and Ph.D. (2015) from Beijing University of Chemical Technology, China. In 2016, He joined Beijing Advanced Innovation Center for Soft Matter Science and Engineering, Beijing University of Chemical Technology as an associate professor. His current scientific interests are focused on the self-assembly of nanoparticles, the supramolecular assemblies and nanocomposites.



Thomas P. Russell the Silvio O. Conte Distinguished Professor of Polymer Science and Engineering at the University of Massachusetts in Amherst, received his PhD in 1979 in Polymer Science and Engineering from the University of Massachusetts Amherst, a Research Associate at the University of Mainz (1979-1981), a Research Staff Member at the IBM Almaden Research Center in San Jose, CA (1981-1996). He is also a Visiting Faculty at the Materials Science Division in the Lawrence

Berkeley National Laboratory, a part-time PI in the Beijing Advanced Innovation Center at the Beijing University of Chemical Technology, and a PI at the Advanced Institute of Materials Research at Tohoku University. His research focuses on the surface and interfacial properties of polymers, thin polymer films, the use of polymers as scaffolds and templates for the generation of nanoscopic structures, the interfacial assembly of nanoparticles, structuring liquids, polymer upcycling, and organic and perovskite-based solar cells.